UM-P-91/102

Description of transitional nuclei in the sdg boson model

V.-S. Lac and S. Kuyucak
School of Physics, University of Melbourne, Parkville, Victoria 3052, Australia

Abstract

We study the transitional nuclei in the framework of the sdg boson model. This extension is necessitated by recent measurements of E2 and E4 transitions in the Pt and Os isotopes which can not be explained in the sd boson models. We show how γ-unstable and triaxial shapes arise from special choices of sdg model Hamiltonians and discuss ways of limiting the number of free parameters through consistency and coherence conditions. A satisfactory description of E2 and E4 properties is obtained for the Pt and Os nuclei, which also predicts dynamic shape transitions in these nuclei.

1. Introduction

Description of transitional nuclei has been one of the most challenging tasks for collective models of nuclei. A complicating feature of these nuclei is the triaxial nature of their energy surface which is neither γ-rigid as in the Davydov-Filippov model [1] nor γ-unstable as in the Wilets-Jean model [2], but rather γ-soft which necessitates introduction of more elaborate geometric models such as the Generalized Collective Model [3]. More recently, the interacting boson model (IBM) [4] has provided a very simple description for the transitional nuclei based on the O(6) limit and its perturbations [5-6]. The O(6) limit had been especially successful in explaining the E2 transitions among the low-lying levels of the Pt isotopes [5-6]. Its main shortcomings are (i) the energy surface is γ-unstable which leads to too much staggering in the quasi-γ band [7], (ii) the quadrupole moments vanish [8], (iii) the B(E2) values fall off too rapidly due to boson cut-off [9], (iv) it fails to describe the E4 properties [10-18]. None of the above problems could be satisfactorily resolved within the standard IBM (i.e. sd bosons with one- and two-body interactions), and the model needs to be extended. The simplest way to do this is to introduce higher order interactions which could be motivated as resulting from the renormalization of g bosons. Although a particular problem could be addressed in this way, e.g., a special choice of cubic interaction introduces a γ-soft component in the energy surface and hence resolves the staggering problem (i) [7]), solution of all the above problems (i)-(iv) in a consistent manner is not easy to achieve. A second extension involves the proton-neutron degree of freedom (IBM-2) which, for example, resolves the quadrupole moment problem (ii) [19]), but fails in other aspects. Another extension, which is strongly suggested by the points (iii) and (iv) above, is to include the g boson.

There is now an extensive set of experimental data indicating the necessity of including the g boson in the IBM calculations (see ref. 5 for a review). However

due to the technical difficulty of diagonalization in a large basis space and the excessive number of parameters (32), progress on the theory side has been slow. So far, applications of the sdg model has been mainly limited to the deformed nuclei where this need is especially acute. Various approximation schemes were used to deal with the large basis problem, e.g., truncating the basis either to a maximum of one g boson [20]) or using an SU(3) basis [21]). Another approach has been the analytical $1/N$ expansion method [22]) which is especially suited to deformed nuclei which have $N < 10$. In the case of the transitional nuclei where the boson numbers are relatively smaller ($N < 10$), an exact diagonalization would be preferable, and is still possible in larger mainframes. The purpose of this paper is to carry out such an exact analysis using the computer code SDGBOSON [23]), and show that within a restricted set of parameters, it is possible to address the problems mentioned above.

In section 2, we discuss a class of sdg model Hamiltoninans suggested by a study of shapes [24]) to be suitable for the transitional nuclei. Parameter dependence of various physical quantities are studied with a view to restrict the number of parameters in a physically meaningful way. The systematics presented in this section would be useful for feature calculations in this region. In section 3, these ideas are used in the calculation of Pt and Os isotopes. Here the emphasis is on those E2 and E4 properties which require explicit introduction of g boson for explanation.

2. sdg model Hamiltonians for transitional nuclei

The sdg model contains far too many parameters (32 in total) for a meaningful analysis of experimental data. Application of the model, therefore, hinges on identification of a simple set of parameters that captures the essential physics. In this process, we are guided by a recent study of shapes [24]) which showed that (i) one-body terms control the spherical to deformed shape transition but have no effect on the

γ degree of freedom, (ii) odd multipole interactions do not play any role on shapes, (iii) quadrupole interaction always leads to an axial shape except when the diagonal terms vanish (q_{ll}=0) which results in a γ-unstable shape, (iv) for certain choices of hexadecapole interaction, one can obtain stable triaxial shapes which are γ-soft. The above points suggest that a Hamiltonian of the form

$$H = \epsilon_g n_g + \kappa_1 L \cdot L + \kappa_2 Q \cdot Q + \kappa_4 T_4 \cdot T_4, \tag{2.1}$$

should be adequate for the description of transitional nuclei. Here the various multipole operators are given by

$$n_g = \sum_\mu g^\dagger_\mu g_\mu, \tag{2.2}$$

$$L_\mu = \sqrt{10}[d^\dagger \tilde{d}]^{(1)}_\mu + \sqrt{60}[g^\dagger \tilde{g}]^{(1)}_\mu, \tag{2.3}$$

$$Q_\mu = [s^\dagger \tilde{d} + d^\dagger \tilde{s}]^{(2)}_\mu + c_{22}[d^\dagger \tilde{d}]^{(2)}_\mu + q_{24}[d^\dagger \tilde{g} + g^\dagger \tilde{d}]^{(2)}_\mu + q_{44}[g^\dagger \tilde{g}]^{(2)}_\mu, \tag{2.4}$$

$$T_{4\mu} = [s^\dagger \tilde{g} + g^\dagger \tilde{s}]^{(4)}_\mu + h_{22}[d^\dagger \tilde{d}]^{(4)}_\mu + h_{24}[d^\dagger \tilde{g} + g^\dagger \tilde{d}]^{(4)}_\mu + h_{44}[g^\dagger \tilde{g}]^{(4)}_\mu. \tag{2.5}$$

This Hamiltonian contains 10 parameters namely, ϵ_g, the single g-boson energy, κ_1, κ_2 and κ_4 which are the strength parameters for the dipole, quadrupole and hexadecapole interactions, and the quadrupole and hexadecapole parameters q_{jl} and h_{jl}. Although it has a substantially lower number of free parameters, a further reduction would be desirable.

We first consider a special case of eq. (2.1) with $q_{22} = q_{44} = \kappa_4 = 0$ which has a a γ-unstable energy surface and hence preserves the successful features of the O(6) limit, such as the well-known O(5) selection rule $\Delta\tau = \pm 1$ for the E2 transitions [25]). In order to illustrate this approximate realization of the O(5) symmetry in the sdg model more quantitatively, we compare the O(6) and sdg model results for $N = 6$ in

table 1. Column 2 shows the O(6) results with $\kappa_1 = 10$ keV, $\kappa_2 = -50$ keV. For the sdg model calculation in the third column, we use the same κ_1, κ_2 and in addition $\epsilon_g = 1000$ keV, $q_{24} = 1$ which are typical values in this region. Note that the sdg energies are consistently lower than the corresponding O(6) energies which suggests an inherent scaling rule. The last column shows such a renormalized sdg calculation with $\kappa_1 = 12.4$ keV, $\kappa_2 = -55$ keV, $\epsilon_g = 1100$ keV, $q_{24} = 1$. The parameters are obtained by scaling the Hamiltonian so that the energies of the 0_2^+ states in column 2 and 3 coincide, and then adjusting κ_1 to obtain the correct splitting between the 4_1^+ and 2_2^+ states. The energies for the $\sigma = N$ levels are seen to agree within one percent. Only the $\sigma = N-2$ (0_3^+, 2_4^+) levels are shifted as a whole by about 100 keV which is the result of the breaking of the O(6) symmetry. In the same table, we also show some of the nonzero E2 matrix elements. Again the renormalized sdg model calculations agree with the O(6) ones within a few percent. Of particular interest here is the transition $0_3^+ \rightarrow 2_1^+$ which is forbidden in the O(6) limit due the selection rule $\Delta\sigma = 0$. In the renormalized calculation, this matrix element is nonzero indicating the breaking of the O(6) symmetry. Nevertheless this value is quite small and lies well within the recently measured experimental upperbound [26]).

As long as ϵ_g is not too small, the above scaling property also holds for other values of q_{24} and ϵ_g. Thus variations in q_{24} and ϵ_g basically preserves the structure of the O(6) limit for the low-lying states (sd-subset), especially in the O(5) sector. In the following, we will keep referring to the sd subset of states with the τ quantum number to facilitate the discussion. Although the O(5) symmetry is not exact, its breaking is quite small and the use of τ as an approximate label is justified.

The above choice of the Hamiltonian shares both the successful features of the O(6) limit and also its failures which stem from the γ-unstable nature of its energy surface. As pointed out in (iv) above, inclusion of a hexadecapole interaction as in eq.

(2.1) could lead to a triaxial shape which is γ-soft. Phenomenological determination of the hexadecapole parameters h_{jl}, however, poses a problem as the E4 data are rather scarce. In order avoid proliferation of parameters, we determine h_{jl} from q_{jl} through a commutation condition which ensures that the quadrupole and the hexadecapole mean fields are coherent [22]). That is, we impose $[\bar{h}, \bar{q}] = 0$ which yields

$$\bar{h}_{22} = \bar{q}_{24}, \;\; \bar{h}_{24} = \bar{q}_{44}, \;\; \bar{h}_{44} = \bar{q}_{24} - (\bar{q}_{44}^2 - \bar{q}_{22}\bar{q}_{44} - 1)/\bar{q}_{24} \; , \tag{2.6}$$

where $\bar{q}_{jl} =< j0l0|20 > q_{jl}$ and $\bar{h}_{jl} =< j0l0|40 > h_{jl}$. When q_{22}=q_{44}=0, eq. (2.6) gives

$$\bar{h}_{22} = \bar{q}_{24}, \;\; \bar{h}_{24} = 0, \;\; \bar{h}_{44} = \bar{q}_{24} - 1/\bar{q}_{24} \; . \tag{2.7}$$

The above choice for h_{jl}, (2.7) automatically satisfies the condition required to induce triaxiality, namely $\bar{h}_{44} < 0$ as $\bar{q}_{24}$ is bound by the SU(3) value of 0.687. The amount of triaxiality (and, hence, the energy staggering in the γ-band) is basically driven by the strength of the hexadecapole interaction in much the same way as the strength of the cubic interaction in the sd model [20]). In fig. 1, we show the effect of such a hexadecapole force on some selected energy levels. In order to isolate the staggering caused by the hexadecapole interaction, we have adjusted κ_1 so that the $\tau = 2$ multiplet (2_2^+, 4_1^+ levels) remains degenerate. The behaviour of the O(6)-like levels is similar to those of the cubic calculations in the sd model [20]). For example, staggering in the γ-band is reduced and the energy splitting in the β band is smaller. Unlike the cubic interaction, however, the hexadecapole interaction strength can not be increased without bound. As shown in fig. 1b, the g boson, 4^+ state rapidly comes down in energy with increasing κ_4 (the kink is due to the mixing of the $\tau = 4$, 4^+ state as they cross over). Thus κ_4 controls not only the amount of triaxiality but more so the positions of the g-boson states, and would be best determined by them.

Apart from inducing triaxiality, this interaction also preserves the E2 selection rules similar to the cubic interaction in the sd model. A consistent E4 operator with the parameters given in eq. (2.7) satisfies selection rules complimentary to the E2 operator i.e. $\Delta\tau = 0, \pm 2$. This has the consequence that the E4($0_1^+ \rightarrow 4_i^+$) matrix elements are large for $i = 1, 4$, and small or vanish for $i = 2, 3$ where $i = 1, 2, 3$ refer to the $\tau = 2, 3, 4$ multiplets in the sd subspace and $i = 4$ denotes the $K = 4^+$ (g boson) band. Therefore, such a consistent E4 operator can explain two of the large matrix elements observed in transitional nuclei. Fig. 2 shows the variation of the ratio E4($0_1^+ \rightarrow 4_4^+$)/E4($0_1^+ \rightarrow 4_1^+$) with q_{24}. The strong dependence of this ratio on q_{24} persists for other (nonzero) values of q_{22} and q_{44} and thus can be used to determine q_{24}. The dependence of this ratio on q_{22} and q_{44} will be examined later in this section.

The Hamiltonians considered in the previous paragraphs showed how various shortcomings of the O(6) limit could be rectified in the sdg model with a limited number (4-5) of parameters. A common feature of these Hamiltonians is that they preserve the E2 selection rules and hence fail to describe the nonvanishing quadrupole moments observed in transitional nuclei. This clearly calls for relaxing the condition $q_{22} = q_{44} = 0$ in the quadrupole operator (2.4). In the following, we consider the Hamiltonian (2.1) with a general quadrupole operator but with the hexadecapole parameters still determined from the condition (2.6). In addition, we will keep using the consistent E2 and E4 operators

$$T(E2) = e_2 Q, \quad T(E4) = e_4 T_4 \tag{2.8}$$

in the calculation of electromagnetic transitions, so that, apart from the effective charges e_2 and e_4, no new parameters are introduced.

In order to give a feeling for the extra parameters, we study their effect on some key physical quantities. First, we consider the quadrupole parameters q_{22} and q_{44} in

the absence of a hexadecapole interaction. Fig. 3a shows the variation of the diagonal E2 matrix element for the first 2^+ state with q_{22}. It has a linear dependence on q_{22} for small values and saturates as q_{22} approaches to its SU(3) value of ± 1.242. Also shown in this figure is the effect of q_{44} which is rather marginal. It is seen to enhance the quadrupole moment slightly when q_{22} and q_{44} have the same signs. Figure 3b shows the E2 ratio $R_g = < 2_1||Q||2_2 > / < 2_1||Q||0_1 >$ as a function of q_{22} for three different values of q_{44}. This ratio is at a maximum near the O(6) limit, decreases linearly with q_{22} and vanishes as q_{22} aproaches to its SU(3) value. Again q_{44} has a small coherent effect on this ratio.

Next, we study the E2 branching ratios from the quasi-γ (fig. 4a) and quasi-β bands (fig. 4b) which indicates how the $\Delta\tau = \pm 1$ selection rule is broken by q_{22} and q_{44}. Both branching ratios have a linear dependence on q_{22} as expected from perturbation theory, and q_{44} has a coherent effect as before. Note, however, the early saturation and the larger role played by q_{44} in the case of the quasi-β band.

Of particular importance are the E4 transitions from the ground state to various 4^+ states which are studied in fig. 5. Here the E4 ratios defined as $R_i = < 0_1||T_4||4_i > / < 0_1||T_4||4_1 >$ for $i = 2, 3, 4$ are plotted against q_{44} for selected values of q_{22}. Note that these ratios do not change under the sign change $(q_{22}, q_{24}, q_{44}) \rightarrow (-q_{22}, q_{24}, -q_{44})$ hence only the negative values of q_{22} are shown. Fig. 5a shows the ratio R_2 which vanishes in the γ-unstable case contrary to experiment. Substantial values for R_2 can be obtained when q_{22} and q_{44} are large and have the the opposite signs. In figs. 5b and 5c, the same ratio is examined for the 4_3^+ ($\tau = 4$) and 4_4^+ (g boson) states. These two states are quite close in energy and, as pointed out earlier (cf. fig. 2), could mix strongly. The inverse parabolic shapes in figs. 5b and 5c simply reflect that this mixing increases with q_{44}. As in the case of R_2, larger values for R_3 and R_4, as demanded by the E4 data, can only be obtained if q_{22} and q_{44} have the opposite

signs.

We next turn to the effects of a hexadecapole interaction with h_{jl} determined from eq. (2.7). The quadrupole parameters are fixed at $(q_{22}, q_{24}, q_{44}) = (0.2, 1, -1)$ as suggested by experimental systematics, and a larger g boson energy, $\epsilon_g = 1000$ keV, is used to counter the effects of an attractive hexadecapole interaction. Fig. 6 shows the energies for the same set of states as in fig. 1 which look very similar except for the g boson 4^+ state. Note however that κ_4 has different signs in the two figures, and the attractive hexadecapole interaction in fig. 6 actually drives the system towards the γ-unstable limit in complete contrast to fig. 1. Thus staggering systematics suggest a repulsive hexadecapole interaction when the parameters h_{jl} are determined from q_{jl}. This move towards the γ-unstable limit with increasing -κ_4 is also apparent from the E2 properties as shown in fig. 7. In fig. 7a, the diagonal E2 matrix element for the 2^+ state is seen to rapidly decrease with -κ_4. Similarly, in fig. 7b, the E2 ratios R_g, R_β and R_γ approach to their limiting values around one and zero (cf. figs. 3 and 4). Finally, fig. 8 shows the E4 ratios as defined in fig. 5. The rapid fall-off in R_4 is due to the change in character of the 4_4^+ state, which starts off as a g boson state for $\kappa_4 < 0$ but mixes with and finally becomes the $\tau = 5$, 4^+ state as the g boson states are pushed up with increasing κ_4 (cf. fig. 6). Otherwise, the E4 ratios show very little dependence on κ_4.

To summarize the systematic studies above, it is possible to describe the E2 and E4 properties with a general quadrupole and a coherent hexadecapole operator in the Hamiltonian if $\kappa_4 < 0$. Although a positive κ_4 is suggested by the staggering sytematics, such a choice destroys the excellent description of the E2 properties (e.g. fig. 7b), and is not preferred. A simultaneous solution of all the problems noted in the introduction obviously requires relaxing one of the coherence or consistency conditions. This would introduce further parameters which we would rather avoid.

As will be seen in the next section (see figs. 9 and 11), energies are reasonably well described with the current set of restricted parameters.

3. Application to Pt and Os isotopes

We now proceed to carry out fits to the Pt and Os data using the insights gained in the preceeding section. Here, we do not attempt to fit each individual nucleus in detail but rather we stress the overall trend. In this way, the number of variable parameters is kept to a minimum. As a result however we anticipate some minor discrepancies between the calculated and experimental results. Further, since the energy of the g boson state ($K = 4^+$ band) is almost constant in the transitional region, the ratio κ_4/ϵ_g is kept approximately constant in each isotopic chain. The three parameters (κ_1,κ_2,κ_4/ϵ_g) are fitted mainly to the lowest-lying bands. The quadrupole parameters (q_{22}, q_{24}, q_{44}) on the other hand are adjusted to fit the E2 and E4 transitions. The parameters are shown in table 2.

3.1. PLATINUM ISOTOPES

We restrict ourselves to a study of $^{192-198}$Pt isotopes for which there are E4 data available. The energy spectra of the Pt isotopes have many features in common. Therefore, we show in fig. 9 ^{194}Pt as a representative example. The calculated spectrum is very similar to that of the perturbed O(6) calculations [6]), and hence shares some of its shortcomings, e.g. staggering in the quasi-γ band and the energy splitting in the quasi-β band are too large. As stressed in the last section, resolution of these problems require additional free parameters which we prefer not to introduce at this stage.

In tables 3-7, we compare the calculated E2 matrix elements with the available data in $^{192-198}$Pt. The boson effective charge e_2 is fixed in each nucleus from the

$E2(2_1^+ \rightarrow 0_1^+)$ transition. In general, the calculated E2 matrix elements agree well with the data, particularly for the stronger E2 transitions which correspond to those allowed by the $\Delta\tau = \pm 1$ selection rule of the O(6) limit. The weaker transitions, which would be forbidden in the O(6) limit, are reasonably well described though discrepancies remain in details. Note that these deviations from the measured values are not uniform (i.e. sometimes smaller and sometimes larger), and hence are not easily rectified in a systematic study with smoothly changing parameters. The most glaring discrepancy occurs for the E2 transitions from the 2_3^+ state in ^{198}Pt. The calculated values are an order of magnitude smaller than the measured ones which results from the persistence of the $\Delta\sigma = 0$ selection rule of the O(6) limit. Further theoretical work on more effective ways of breaking the O(6) symmetry is needed to address this problem. Also, further experimental study of the E2 transition from the $\sigma = N - 2$ levels would be desirable to shed more light on systematics.

The inability of the sd models to describe the E2 transitions along the yrast band due to the boson cut-off at $L = 2N$ was recently stressed [9]). In the sdg model, the boson cut-off is pushed to $L = 4N$, and as a result, agreement with the experiment is recovered (see tables 3-7). Also shown in these tables are the diagonal E2 matrix elements which are fairly well described. In order to depict the systematics better, the quadrupole moments of the 2_1^+ states are plotted in fig. 10, and seen to agree well with the experimental moments. An interesting feature of the present calculations is that they predict a drop in the quadrupole moments with increasing spin with an eventual change of sign. Such dynamic shape transitions had been predicted to occur in transitional nuclei at spins $L = 10-20$ [27]). The data in ^{196}Pt seem to support such a reduction, however more precise measurements at higher spins would be needed to reach a definite conclusion.

Finally we discuss the E4 transitions which are one of the main motivations for

the present study. Since there are only a few transitions known in each isotope, we prefer to keep the effective charge constant at $e_4 = 0.046\ eb^2$ for all Pt isotopes. Table 7 compares the E4 matrix elements calculated using the consistent E4 operator (2.8) with the available experimental data. Considering that the E4 operator is derived from that of E2, the overall agreement between the calculations and various measurements is excellent. Note that the E4 data on ^{192}Pt are extracted from the less reliable (α, α') experiments [11]), and could be revised in future experiments.

After the completion of the present work, new data on Pt isotopes became available which included the E4 transition to the 4_3^+ ($\tau = 4$) state in ^{196}Pt [17]). The calculated value, 0.065 eb^2, is in very good agreement with the measured value of 0.067 (6) eb^2.

3.2. OSMIUM ISOTOPES

Here we discuss $^{188-192}$Os for which there are E4 data. Fig. 11 shows an example of calculated spectrum for ^{190}Os. Compared to ^{194}Pt (cf. fig. 9), the agreement between the calculated and the experimental level schemes has visibly improved. This happens because the Os isotopes are more deformed than the Pt isotopes and hence the undesired effects of the γ-unstable limit on the energies of the quasi-β and quasi-γ bands are considerably reduced. Another significant change is the lower lying 4^+ (g boson) state which requires a smaller g boson energy (see table 2). Thus the g boson mixing in the sd states is stronger in the Os isotopes and is expected to play a more important role in the spectroscopy of the low-lying states.

Tables 8-10 show a comparison of the E2 matrix elements. Again, compared to the Pt isotopes, the overall agreement is much better with fewer discrepancies. Worth noting here are the E2 transitions from the 4_3^+ (g boson) state which are fairly well

described. If the g bosons were weakly coupled, these transitions would be small and such a successful description would not have been possible.

The quadrupole moments of the 2_1^+ states are shown fig. 10, and agree well with the experiments. The drop in the quadrupole moments with increasing spin, which was encountered in the Pt isotopes, also happens in the Os isotopes. In fig. 12, we show the quadrupole moment calculations up to high spins which predict a prolate-oblate shape transition around $L = 16$. The available data have rather large error bars, and more precise measurements extending to higher spins would be desirable.

Unlike the Pt isotopes, the E4 information on the Os isotopes is less complete (table 10). The (p, p') experiments are so far carried out only for ^{192}Os [15]), and the E4 data are fairly well described in this case. The other E4 data for the E4$(0_1^+ \rightarrow 4_3^+)$ transitions come from (α, α') experiments which are sensitive to the details of the reactions and are therefore less reliable. The E4$(0_1^+ \rightarrow 4_1^+)$ transitions on the other hand are extracted from the more reliable (e, e') experiments, and are quite well reproduced in the calculations.

4. Summary and conclusions

We have discussed in this paper some special features of the sdg boson model which are relevant to the description of transitional nuclei. In particular, we have shown how the γ-unstable limit can be obtained from a quadrupole Hamiltonian, and how a coherent hexadecapole interaction can induce a γ-soft triaxiality. We have also considered the model Hamiltonian in more general terms and produced systematic trends for various physical quantities of interest.

An overbearing concern in the sdg model is the number of free parameters. Through various consistency and coherence conditions, we have restricted this number to nine (7 in the Hamiltonian and two effective charges), which are mostly held

constant or change smoothly within an isotopic chain. Considering that 30-40 pieces of data are explained for each nucleus, this roughly doubling of the parameters compared to the sd model is well justified. It should also be emphasized that some of the E2 and E4 data can not be described without the g bosons regardless of the number of parameters used in the sd models.

In summary, a consistent description of the E2 and E4 properties in the Pt and Os isotopes has been obtained using a restricted set of parameters. The problems with the quadrupole moments, yrast E2 and E4 transitions, which can not be explained in the sd models, have been satisfactorily resolved. An interesting prediction of the present calculations is the dynamic shape transitions which could be tested with the new 4π-detector systems "Euroball" and "Gamma-Sphere".

Finally, the Xe-Ba region shows very similar characteristics, and the sdg model can also be applied to these nuclei. We refrained from doing so here because the choice of the model parameters depends sensitively on the E4 data which are lacking at the moment. We therefore emphasize the importance of E4 measurements in pinning down the hexadecapole features, and strongly suggest (e,e') and/or (p,p') experiments in the Xe-Ba region.

This work was supported by an Australian Research Council grant. We thank Drs. D.G. Burke, A. Sethi, F. Todd Baker and H.J. Wollersheim for useful discussions and communications regarding the recent E2 and E4 data.

REFERENCES

[1] A.S. Davydov and G.F. Filippov, Nucl. Phys. **8** (1958) 237

[2] L. Wilets and M. Jean, Phys. Rev. **102** (1956) 788

[3] G. Gneuss and W. Greiner, Nucl. Phys. **A171** (1971) 449; P.O. Hess, J.Maruhn and W. Greiner, J. Phys. **G7** (1981) 737.

[4] F. Iachello and A. Arima, The interacting boson model (Cambridge U.P., Cambridge, 1987)

[5] R.F. Casten and D.D. Warner, Rev. Mod. Phys. **60** (1988) 389

[6] R.F. Casten and J.A. Cizewski, Nucl.Phys. **A309** (1978) 477; Phys. Lett. **B185** (1987) 293

[7] R.F. Casten, P. von Brentano, K. Heyde, P. van Isacker and J.Jolie, Nucl. Phys. **A439** (1985) 289

[8] M.P. Fewell, et al., Phys. Lett. **B157** (1985) 353; M.P. Fewell, Phys. Lett. **B167** (1986) 6

[9] A. Mauthofer, et al., Z. Phys. **A336** (1990) 263

[10] D.G. Burke, M.A.M. Shahabudin and R.N. Boyd, Phys. Lett. **B78** (1978) 48

[11] F. Todd Baker, et al., Phys. Rev. **C17** (1978) 1559

[12] P.T. Deason, et al., Phys. Rev. **C23** (1981) 1414

[13] W.T.A. Borghols, et al., Phys. Lett. **B152** (1985) 330

[14] W. Boeglin, et al., Nucl. Phys. **A477** (1988) 399

[15] F. Todd Baker, et al., Nucl. Phys. **A501** (1989) 546

[16] A. Sethi, et al., Nucl. Phys. **A518** (1990) 536

[17] A. Sethi, et al., Phys. Rev. **C44** (1991) 700

[18] A. Sethi, Private communication, (1991)

[19] R. Bijker, A.E.L. Dieperink, O. Scholten and R. Spanhoff, Nucl. Phys. **A344** (1980) 207

[20] P. Van Isacker, K. Heyde, M. Waroquier and G. Wenes, Nucl. Phys. **A380** (1982) 383

[21] N. Yoshinaga, Y. Akiyama and A. Arima, Phys. Rev. **C38** (1988) 419

[22] S. Kuyucak and I. Morrison, Ann. Phys. (NY) **181** (1988) 79; S. Kuyucak, I. Morrison and T. Sebe, Phys. Rev. **C43** (1991) 1187

[23] I. Morrison, Computer code SDGBOSON, (University of Melbourne, 1986)

[24] S. Kuyucak and I. Morrison, Phys. Lett. **B255** (1991) 305

[25] S. Kuyucak, V.-S. Lac, I. Morrison and B.R. Barrett, Phys. Lett. **B263** (1991) 347

[26] H.G. Börner, J. Jolie, S. Robinson, R.F. Casten and J.A. Cizewski, Phys. Rev. **C42** (1990) R2271

[27] S. Kuyucak, V.-S. Lac and I. Morrison, Phys. Lett. **B263** (1991) 146

[28] H.H. Bolotin, A.E. Stuchbery, I. Morrison, D.L. Kennedy, C.G. Ryan and S.H. Sie, Nucl. Phys. **A370** (1981) 146

[29] P. Raghavan, Atomic Data and Nuclear Data Tables **42** (1989) 189

[30] B. Singh, Nuclear Data Sheets **56** (1989) 124.

[31] C.Y. Wu, Ph. D. thesis, (University of Rochester, 1983)

[32] L. Yabo, H. Dailing, S. Hueibin and D. Zhaozhong, Z. Phys. **A329** (1988) 307

[33] E. Eid and N.M. Stewart, Z. Phys. **A320** (1985) 495

[34] N.R. Johnson, Phys. Rev. **C15** (1977) 1325

[35] B. Singh, Nuclear Data Sheets **61** (1990) 243

[36] B. Singh, Nuclear Data Sheet, **59** (1990) 133

TABLE CAPTIONS

TABLE 1. Comparison of energies and E2 matrix elements for the O(6), sdg and renormalized sdg model calculations. See text for the parameters.

TABLE 2. Parameters used in the sdg calculations.

TABLE 3. Comparison of E2 matrix elements for ^{198}Pt.

TABLE 4. Comparison of E2 matrix elements for ^{196}Pt.

TABLE 5. Comparison of E2 matrix elements for ^{194}Pt.

TABLE 6. Comparison of E2 matrix elements for ^{192}Pt.

TABLE 7. Comparison of E4 matrix elements. The effective E4 charges are $e_4 = 0.0461eb^2$ for platinum isotopes (determined from fitting the $0_1^+ \rightarrow 4_1^+$ transition in ^{196}Pt), and $e_4 = 0.0343eb^2$ for osmium isotopes (determined from fitting the $0_1^+ \rightarrow 4_1^+$ transition in ^{192}Os). 4_g^+ denotes the g boson state which could be the third or fourth 4^+ state depending on the nucleus.

TABLE 8. Comparison of E2 matrix elements for ^{192}Os.

TABLE 9. Comparison of E2 matrix elements for ^{190}Os.

TABLE 10. Comparison of E2 matrix elements for ^{188}Os.

TABLES

TABLE 1.

	O(6)	sdg	ren. sdg
0_1^+	0	0	0
2_1^+	260	226	258
2_2^+	560	498	556
4_1^+	700	607	696
0_2^+	900	819	900
3_1^+	1020	911	1018
4_2^+	1100	973	1098
6_1^+	1320	1146	1320
0_3^+	1400	1371	1506
2_4^+	1660	1598	1764
$2_1^+ \rightarrow 0_1^+$	7.75	8.11	7.75
$2_2^+ \rightarrow 2_1^+$	8.86	9.33	8.91
$4_1^+ \rightarrow 2_1^+$	11.89	12.67	12.10
$0_3^+ \rightarrow 2_1^+$	0	0.07	0.06

TABLE 2.

		Strength parameters (keV)				Quadrupole parameters		
Nucleus	N	κ_1	κ_2	κ_4	ϵ_g	q_{22}	q_{24}	q_{44}
^{198}Pt	5	21.0	-50.0	-18.0	1000	0.21	0.80	-1.00
^{196}Pt	6	18.0	-49.0	-18.0	1000	0.20	0.80	-1.00
^{194}Pt	7	16.0	-48.5	-18.0	1000	0.18	0.80	-1.00
^{192}Pt	8	15.0	-47.5	-18.0	1000	0.17	0.80	-1.00
^{192}Os	8	15.0	-30.0	-12.0	500	-0.24	0.90	0.50
^{190}Os	9	12.5	-34.0	-13.0	540	-0.26	0.90	0.50
^{188}Os	10	5.5	-40.0	-15.0	630	-0.28	0.90	0.50

TABLE 3.

$J_i \rightarrow J_f$	$\mid < J_f \mid\mid \mathrm{T(E2)} \mid\mid J_i > \mid_{calc.}$	$\mid < J_f \mid\mid \mathrm{T(E2)} \mid\mid J_i > \mid_{exp.}$ Value	Reference
$2_1^+ \rightarrow 0_1^+$	1.010	1.010 ± 0.050	28
$4_1^+ \rightarrow 2_1^+$	1.565	1.559 ± 0.066	28
$6_1^+ \rightarrow 4_1^+$	1.919	≥ 2.266	28
$2_2^+ \rightarrow 2_1^+$	1.041	1.145 ± 0.083	28
		0.962 ± 0.062	28
$2_2^+ \rightarrow 0_1^+$	0.108	0.039 ± 0.006	28
$0_2^+ \rightarrow 2_1^+$	0.079	0.437 ± 0.058	28
$2_3^+ \rightarrow 2_2^+$	0.075	0.846 ± 0.334	28
$2_3^+ \rightarrow 2_1^+$	0.002	0.141 ± 0.044	28
$2_1^+ \rightarrow 2_1^+$	0.514	0.554 ± 0.158	29
		0.712 ± 0.158	29

e_2=0.148 eb.

TABLE 4.

$J_i \rightarrow J_f$	$\lvert < J_f \lVert \mathrm{T(E2)} \rVert J_i > \rvert_{calc.}$	$\lvert < J_f \lVert \mathrm{T(E2)} \rVert J_i > \rvert_{exp.}$ Value	Reference
$2_1^+ \rightarrow 0_1^+$	1.200	1.200 ± 0.029	28
$4_1^+ \rightarrow 2_1^+$	1.881	1.904 ± 0.076	28
		$1.997\ (^{+0.070}_{-0.047})$	9
$6_1^+ \rightarrow 4_1^+$	2.345	2.339 ± 0.322	28
		$2.534\ (^{+0.056}_{-0.133})$	9
$8_1^+ \rightarrow 6_1^+$	2.660	$3.132(^{+0.149}_{-0.166})$	9
$2_2^+ \rightarrow 2_1^+$	1.230	1.323 ± 0.059	28
		$1.145\ (^{+0.122}_{-0.118})$	9
$2_2^+ \rightarrow 0_1^+$	0.148	< 0.003	6
$0_2^+ \rightarrow 2_2^+$	0.612	0.377 ± 0.102	28
$0_2^+ \rightarrow 2_1^+$	0.086	0.148 ± 0.034	28
		$0.182\ (^{+0.014}_{-0.025})$	9
$4_2^+ \rightarrow 4_1^+$	1.239	1.318 ± 0.331	28
		$1.401\ (^{+0.254}_{-0.090})$	9
$4_2^+ \rightarrow 2_2^+$	1.337	1.262 ± 0.125	28
		$1.401\ (^{+0.077}_{-0.212})$	9
$4_2^+ \rightarrow 2_1^+$	0.062	0.164 ± 0.027	28
		$0.144\ (^{+0.019}_{-0.031})$	9
$6_2^+ \rightarrow 6_1^+$	1.206	$1.051\ (^{+1.014}_{-0.482})$	9
$6_2^+ \rightarrow 4_2^+$	1.801	$2.133\ (^{+0.369}_{-0.253})$	9
$6_2^+ \rightarrow 4_1^+$	0.129	$0.219\ (^{+0.050}_{-0.044})$	9
$2_3^+ \rightarrow 2_1^+$	0.006	$0.067\ (^{+0.030}_{-0.011})$	9
$0_3^+ \rightarrow 2_1^+$	0.052	< 0.184	26
$2_1^+ \rightarrow 2_1^+$	0.671	0.871 ± 0.158	29
		0.810 ± 0.230	9
$4_1^+ \rightarrow 4_1^+$	0.577	$0.389\ (^{+0.302}_{-0.322})$	9
$6_1^+ \rightarrow 6_1^+$	0.412	$0.176\ (^{+0.749}_{-0.794})$	9
$8_1^+ \rightarrow 8_1^+$	0.203	$0.227\ (^{+0.903}_{-1.344})$	9
$2_2^+ \rightarrow 2_2^+$	0.627	$0.303\ (^{+0.258}_{-0.455})$	9

e_2=0.151 eb.

TABLE 5.

$J_i \rightarrow J_f$	$\lvert < J_f \lvert\lvert$ T(E2) $\rvert\rvert J_i > \rvert_{calc.}$	$\lvert < J_f \lvert\lvert$ T(E2) $\rvert\rvert J_i > \rvert_{exp.}$ Value	Reference
$2_1^+ \rightarrow 0_1^+$	1.284	1.284 ± 0.006	30
$4_1^+ \rightarrow 2_1^+$	2.025	1.987 ± 0.038	30
$6_1^+ \rightarrow 4_1^+$	2.550	2.893 ± 0.140	30
$8_1^+ \rightarrow 6_1^+$	2.933	3.205 ± 0.304	30
$2_2^+ \rightarrow 2_1^+$	1.335	1.478 ± 0.027	30
$2_2^+ \rightarrow 0_1^+$	0.160	0.089 ± 0.002	30
$0_2^+ \rightarrow 2_2^+$	0.678	0.235 ± 0.064	30
$0_2^+ \rightarrow 2_1^+$	0.085	0.067 ± 0.019	30
$4_2^+ \rightarrow 4_1^+$	1.365	1.500 ± 0.180	30
$4_2^+ \rightarrow 2_2^+$	1.470	1.775 ± 0.070	30
$4_2^+ \rightarrow 2_1^+$	0.079	0.220 ± 0.017	30
$6_2^+ \rightarrow 6_1^+$	1.369	1.140 ± 0.342	30
$6_2^+ \rightarrow 4_2^+$	2.023	2.078 ± 0.195	30
$6_2^+ \rightarrow 4_1^+$	0.171	0.224 ± 0.032	30
$2_1^+ \rightarrow 2_1^+$	0.707	0.633 ± 0.185	29
		0.831 ± 0.079	29
		$0.540\ (^{+0.081}_{-0.059})$	31
$4_1^+ \rightarrow 4_1^+$	0.593	$1.000\ (^{+0.120}_{-0.140})$	31
$6_1^+ \rightarrow 6_1^+$	0.405	$0.280\ (^{+0.120}_{-0.269})$	31
$2_2^+ \rightarrow 2_2^+$	0.670	0.66 ± 0.66	29
		$0.400\ (^{+0.120}_{-0.052})$	31
$4_2^+ \rightarrow 4_2^+$	0.449	$0.070\ (^{+0.140}_{-0.140})$	31

e_2=0.142 *eb.*

TABLE 6.

$J_i \rightarrow J_f$	$\mid < J_f \mid\mid \mathrm{T(E2)} \mid\mid J_i > \mid_{calc.}$	$\mid < J_f \mid\mid \mathrm{T(E2)} \mid\mid J_i > \mid_{exp.}$ Value	Reference
$2_1^+ \rightarrow 0_1^+$	1.449	1.449 ± 0.035	32,33
$4_1^+ \rightarrow 2_1^+$	2.294	2.343 ± 0.038	32
		2.362 ± 0.057	33
$6_1^+ \rightarrow 4_1^+$	2.908	2.472 ± 0.473	34
$2_2^+ \rightarrow 2_1^+$	1.518	2.179 ± 0.080	32
		1.517 ± 0.082	33
$2_2^+ \rightarrow 0_1^+$	0.183	0.152 ± 0.008	32
		0.148 ± 0.008	33
$3_1^+ \rightarrow 4_1^+$	1.091	1.058 ± 0.099	32
		1.212 ± 0.087	33
$3_1^+ \rightarrow 2_2^+$	1.762	1.962 ± 0.125	32
		1.735 ± 0.121	33
$3_1^+ \rightarrow 2_1^+$	0.277	0.163 ± 0.009	32
		0.179 ± 0.012	33
$2_1^+ \rightarrow 2_1^+$	0.797	0.818 ± 0.079	29
		0.726 ± 0.277	29

e_2=0.144 eb.

TABLE 7.

Nucleus	$E4(0_1^+ \rightarrow 4_1^+)$ Calc.	$E4(0_1^+ \rightarrow 4_1^+)$ Exp.	$E4(0_1^+ \rightarrow 4_2^+)$ Calc.	$E4(0_1^+ \rightarrow 4_2^+)$ Exp.	$E4(0_1^+ \rightarrow 4_g^+)$ Calc.	$E4(0_1^+ \rightarrow 4_g^+)$ Exp.
^{198}Pt	0.150	0.217(7)[a]	0.129	0.188(7)[a]	0.223	0.138(14)[a]
		0.144(3)[c]		0.124(6)[c]		0.094(7)[c]
		0.176[d]		0.207[d]		-
^{196}Pt	0.175	0.175(7)[b]	0.135	0.157(9)[b]	0.243	0.200(5)[b]
		0.155(16)[e]		0.141(14)[e]		0.210(31)[e]
		0.202[d]		0.141[d]		-
		0.131(7)[f]		-		-
^{194}Pt	0.203	0.195(7)[a]	0.140	0.115(7)[a]	0.260	0.229(7)[a]
		0.191(9)[b]		0.131(6)[b]		0.280(10)[b]
		0.132(3)[c]		0.066(11)[c]		0.159(4)[c]
		0.155[d]		0.118[d]		-
		0.175(16)[f]		0.039(3)[f]		-
^{192}Pt	0.230	0.202[g]	0.146	0.20/0.34[g]	0.262	-
^{192}Os	0.196	0.196(11)[h]	0.144	0.116(29)[h]	0.170	0.108(27)[h]
		0.220(10)[f]		-		0.071/0.058[i]
^{190}Os	0.206	0.212(12)[f]	0.163	-	0.163	0.078/0.067[i]
^{188}Os	0.215	0.217(11)[f]	0.181	-	0.159	0.109/0.094[i]

[a] (p,p') experiment [ref. 18], [b] (p,p') experiment [ref. 17], [c] (p,p') experiment [ref. 16], [d] (p,p') experiment [ref. 12], [e] (e,e') experiment [ref. 13], [f] (e,e') experiment [ref. 14], [g] (α,α') experiment [ref 11], [h] (p,p') experiment [ref. 15], [i] (α,α') experiment [ref. 10].

TABLE 8.

$J_i \rightarrow J_f$	$\mid < J_f \mid\mid \mathrm{T(E2)} \mid\mid J_i > \mid_{calc.}$	$\mid < J_f \mid\mid \mathrm{T(E2)} \mid\mid J_i > \mid_{exp.}$ Value	Reference
$2_1^+ \rightarrow 0_1^+$	1.457	1.457 ± 0.018	31
$4_1^+ \rightarrow 2_1^+$	2.330	$2.115\ (^{+0.038}_{-0.044})$	31
$6_1^+ \rightarrow 4_1^+$	2.960	$2.93\ (^{+0.10}_{-0.08})$	31
$8_1^+ \rightarrow 6_1^+$	3.445	$3.58\ (^{+0.17}_{-0.15})$	31
$2_2^+ \rightarrow 2_1^+$	1.231	$1.224\ (^{+0.030}_{-0.016})$	31
$2_2^+ \rightarrow 0_1^+$	0.289	$0.425\ (^{+0.008}_{-0.014})$	31
$2_2^+ \rightarrow 4_1^+$	0.203	$0.35\ (^{+0.12}_{-0.07})$	31
$0_2^+ \rightarrow 2_1^+$	0.152	$0.066\ (^{+0.012}_{-0.013})$	31
$0_2^+ \rightarrow 2_2^+$	0.689	$0.449\ (^{+0.044}_{-0.056})$	31
$4_2^+ \rightarrow 4_1^+$	1.327	$1.35\ (^{+0.10}_{-0.08})$	31
$4_2^+ \rightarrow 2_2^+$	1.562	1.637 ± 0.050	31
$4_2^+ \rightarrow 2_1^+$	0.098	$0.125\ (^{+0.018}_{-0.010})$	31
$4_2^+ \rightarrow 6_1^+$	0.298	$0.40\ (^{+0.20}_{-0.18})$	31
$6_2^+ \rightarrow 6_1^+$	1.324	$1.49\ (^{+0.30}_{-0.20})$	31
$6_2^+ \rightarrow 4_2^+$	2.270	$2.09\ (^{+0.13}_{-0.17})$	31
$6_2^+ \rightarrow 4_1^+$	0.262	0.067 ± 0.076	31
$4_3^+ \rightarrow 4_2^+$	0.583	1.19 ± 0.22	31
$4_3^+ \rightarrow 3_1^+$	0.836	$1.63\ (^{+0.20}_{-0.36})$	31
$4_3^+ \rightarrow 2_2^+$	0.694	$0.79\ (^{+0.12}_{-0.14})$	31
$4_3^+ \rightarrow 2_1^+$	0.153	$0.113\ (^{+0.064}_{-0.046})$	31
$2_1^+ \rightarrow 2_1^+$	1.25	1.21 ± 0.18	31
$4_1^+ \rightarrow 4_1^+$	1.20	$0.73\ (^{+0.15}_{-0.10})$	31
$6_1^+ \rightarrow 6_1^+$	1.05	$1.16\ (^{+0.24}_{-0.34})$	31
$8_1^+ \rightarrow 8_1^+$	0.84	$1.13\ (^{+0.48}_{-0.66})$	31
$10_1^+ \rightarrow 10_1^+$	0.61	(-2.3 -0.4)	31
$2_2^+ \rightarrow 2_2^+$	1.18	0.98 ± 0.10	31

e_2=0.144 eb.

TABLE 9.

$J_i \rightarrow J_f$	$\lvert < J_f \lVert$ T(E2) $\rVert J_i > \rvert_{calc.}$	$\lvert < J_f \lVert$ T(E2) $\rVert J_i > \rvert_{exp.}$ Value	Reference
$2_1^+ \rightarrow 0_1^+$	1.539	1.539 ± 0.013	35
$4_1^+ \rightarrow 2_1^+$	2.476	2.366 ± 0.042	35
$6_1^+ \rightarrow 4_1^+$	3.152	2.970 ± 0.515	35
$8_1^+ \rightarrow 6_1^+$	3.688	3.712 ± 0.105	35
$2_2^+ \rightarrow 2_1^+$	1.123	1.095 ± 0.030	35
$2_2^+ \rightarrow 0_1^+$	0.344	0.456 ± 0.012	35
$0_2^+ \rightarrow 2_2^+$	0.695	0.387 ± 0.032	35
$0_2^+ \rightarrow 2_1^+$	0.156	0.118 ± 0.011	35
$4_2^+ \rightarrow 4_1^+$	1.291	1.439 ± 0.031	35
$4_2^+ \rightarrow 2_2^+$	1.623	1.871 ± 0.040	35
$4_2^+ \rightarrow 2_1^+$	0.056	0.202 ± 0.007	35
$6_2^+ \rightarrow 6_1^+$	1.331	1.766 ± 0.184	35
$6_2^+ \rightarrow 4_2^+$	2.425	2.598 ± 0.156	35
$6_2^+ \rightarrow 4_1^+$	0.259	0.194 ± 0.090	35
$4_3^+ \rightarrow 4_2^+$	0.695	1.587 ± 0.113	35
$4_3^+ \rightarrow 3_1^+$	0.906	$1.543\ (^{+0.091}_{-0.340})$	35
$4_3^+ \rightarrow 2_2^+$	0.781	0.775 ± 0.065	35
$4_3^+ \rightarrow 2_1^+$	0.125	0.052 ± 0.006	35
$4_3^+ \rightarrow 4_1^+$	0.231	≈ 0.199	35
$2_1^+ \rightarrow 2_1^+$	1.497	1.557 ± 0.040	29
		1.253 ± 0.396	29
$2_2^+ \rightarrow 2_2^+$	1.414	1.187 ± 0.528	29

e_2=0.137 *eb*.

TABLE 10.

$J_i \rightarrow J_f$	$\lvert < J_f \lVert \mathrm{T(E2)} \rVert J_i > \rvert_{calc.}$	$\lvert < J_f \lVert \mathrm{T(E2)} \rVert J_i > \rvert_{exp.}$ Value	Reference
$2_1^+ \rightarrow 0_1^+$	1.584	1.584 ± 0.022	36
$4_1^+ \rightarrow 2_1^+$	2.556	2.646 ± 0.057	36
$6_1^+ \rightarrow 4_1^+$	3.257	3.314 ± 0.109	36
$8_1^+ \rightarrow 6_1^+$	3.823	3.950 ± 0.329	36
$2_2^+ \rightarrow 2_1^+$	0.991	0.866 ± 0.023	36
$2_2^+ \rightarrow 0_1^+$	0.374	0.483 ± 0.010	36
$0_2^+ \rightarrow 2_1^+$	0.149	0.077 ± 0.029	36
$4_2^+ \rightarrow 4_1^+$	1.208	1.098 ± 0.090	36
$4_2^+ \rightarrow 2_2^+$	1.623	1.775 ± 0.113	36
$4_2^+ \rightarrow 2_1^+$	0.004	0.283 ± 0.018	36
$6_2^+ \rightarrow 6_1^+$	1.278	1.442 ± 0.406	36
$6_2^+ \rightarrow 4_2^+$	2.505	2.456 ± 0.274	36
$6_2^+ \rightarrow 4_1^+$	0.227	0.127 ± 0.025	36
$4_3^+ \rightarrow 4_2^+$	0.607	1.643 ± 0.246	36
$4_3^+ \rightarrow 2_2^+$	0.853	0.837 ± 0.149	36
$2_1^+ \rightarrow 2_1^+$	1.662	1.926 ± 0.053	29
		1.517 ± 0.330	29
$2_2^+ \rightarrow 2_2^+$	1.571	1.319 ± 0.330	29

e_2=0.128 eb.

FIGURES

FIG. 1. Effect of the hexadecapole interaction on energies. The parameters are $N = 7$, $\kappa_2 = -50$ keV, $q_{24} = 1$, and $\epsilon_g = 500$ keV.

FIG. 2. Variation of the E4 ratio, $R_4 = < 0_1||T_4||4_4 > / < 0_1||T_4||4_1 >$, as a function of q_{24}. Here $\kappa_4 = 0$ and the other parameters are the same as in Fig. 1.

FIG. 3. Diagonal E2 reduced matrix element and the E2 ratio, $R_g = < 2_1||Q||2_2 > / < 2_1||Q||0_1 >$, as a function of q_{22}. The parameters are N=6, $\kappa_1 = 10$ keV, $\kappa_2 = -50$ keV, $\kappa_4 = 0$, $\epsilon_g = 500$ keV and $q_{24} = 1$.

FIG. 4. E2 branching ratios, $R_\gamma = < 2_2||Q||0_1 > / < 2_2||Q||2_1 >$ and $R_\beta = < 0_2||Q||2_1 > / < 0_2||Q||2_2 >$, as a function of q_{22}. The parameters are the same as in Fig. 3.

FIG. 5. E4 ratios, $R_i = < 0_1||T_4||4_i > / < 0_1||T_4||4_1 >$, i=2,3,4, as a function of q_{44}. The parameters are the same as in Fig. 3.

FIG. 6. Energy variations as a function of κ_4. The parameters are $N = 7$, $\kappa_2 = -50$ keV, $\epsilon_g = 1000$ keV and $(q_{22}, q_{24}, q_{44}) = (0.2, 1, -1)$.

FIG. 7. Diagonal E2 reduced matrix element and E2 ratios, R_g, R_γ and R_β as defined in figs 3 and 4, as a function of κ_4. The parameters are the same as in Fig. 6.

FIG. 8. E4 ratios, R_i as defined in fig. 5, as a function of κ_4. The parameters are the same as in Fig. 6.

FIG. 9. Energy levels of ^{194}Pt compared with the sdg model calculations.

FIG. 10. Comparison between the calculated and experimental values for the quadrupole moment of the 2_1^+ state. The experimental values are taken from ref. 29.

FIG. 11. Energy levels of ^{190}Os compared with the sdg model calculations.

FIG. 12. Comparison between the calculated and experimental values for the quadrupole moment of the yrast states in ^{192}Os. The experimental values are taken from ref. 31.

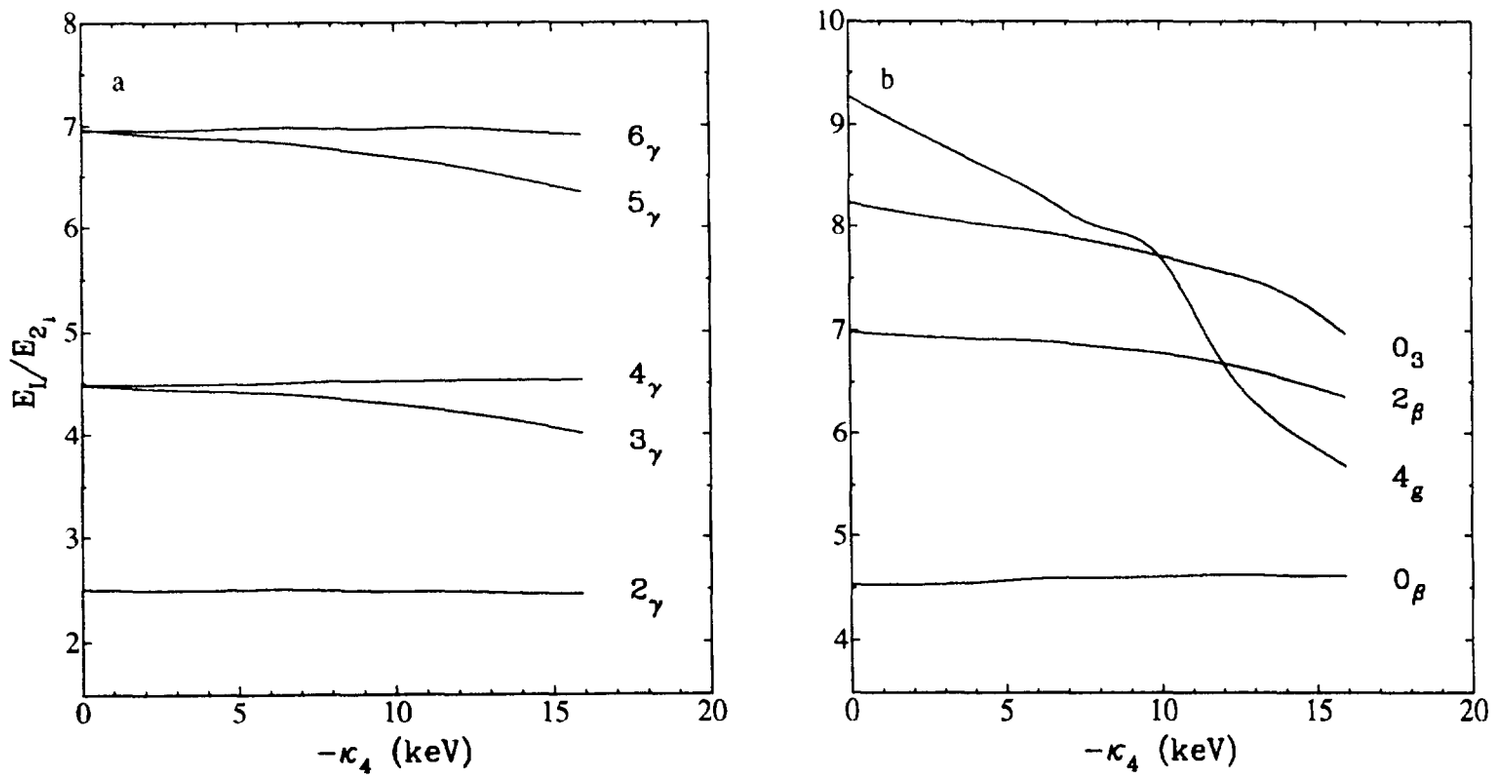
a
b
E_I/E_{2_1}
$-\kappa_4$ (keV)
$-\kappa_4$ (keV)
6_γ
5_γ
4_γ
3_γ
2_γ
0_3
2_β
4_g
0_β

Fig. 1

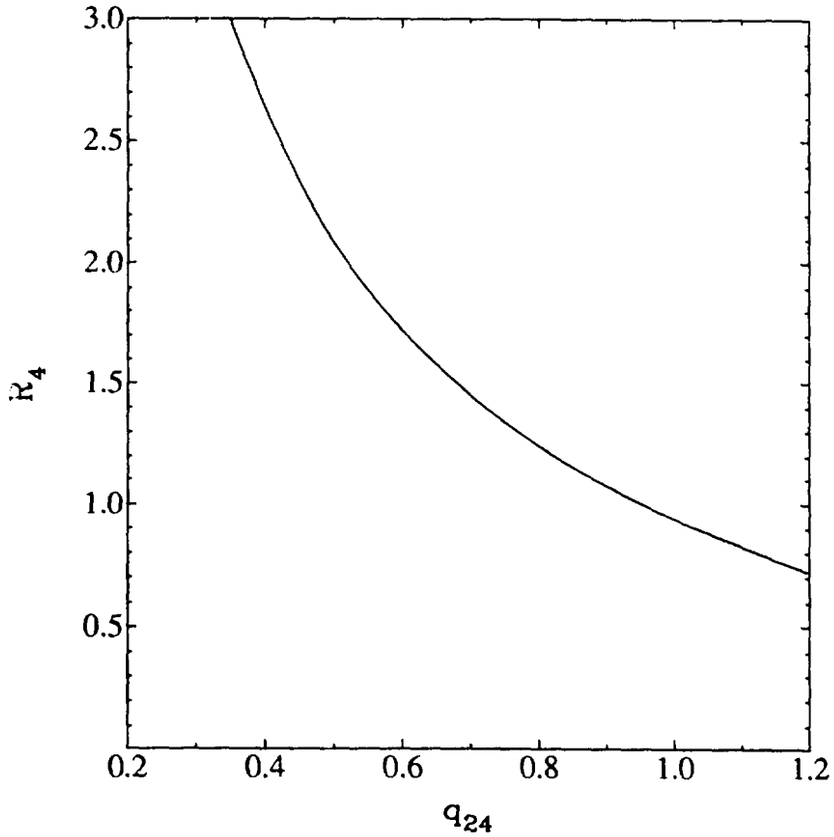

Fig. 2

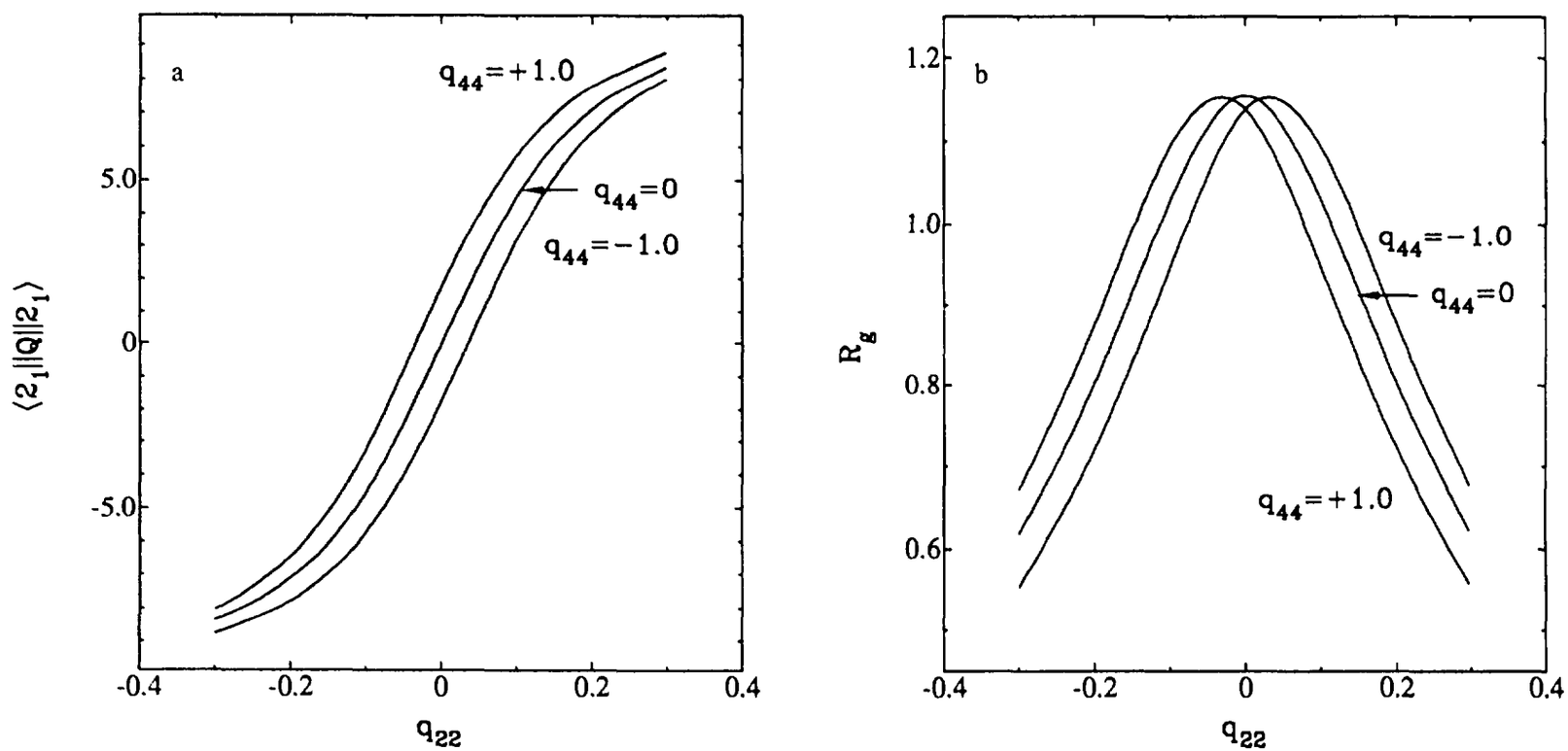
a
$q_{44}=+1.0$
$q_{44}=0$
$q_{44}=-1.0$
$\langle 2_1||Q||2_1\rangle$
5.0
0
-5.0
-0.4
-0.2
0
0.2
0.4
q_{22}
b
$q_{44}=-1.0$
$q_{44}=0$
$q_{44}=+1.0$
R_g
1.2
1.0
0.8
0.6
-0.4
-0.2
0
0.2
0.4
q_{22}

Fig. 3

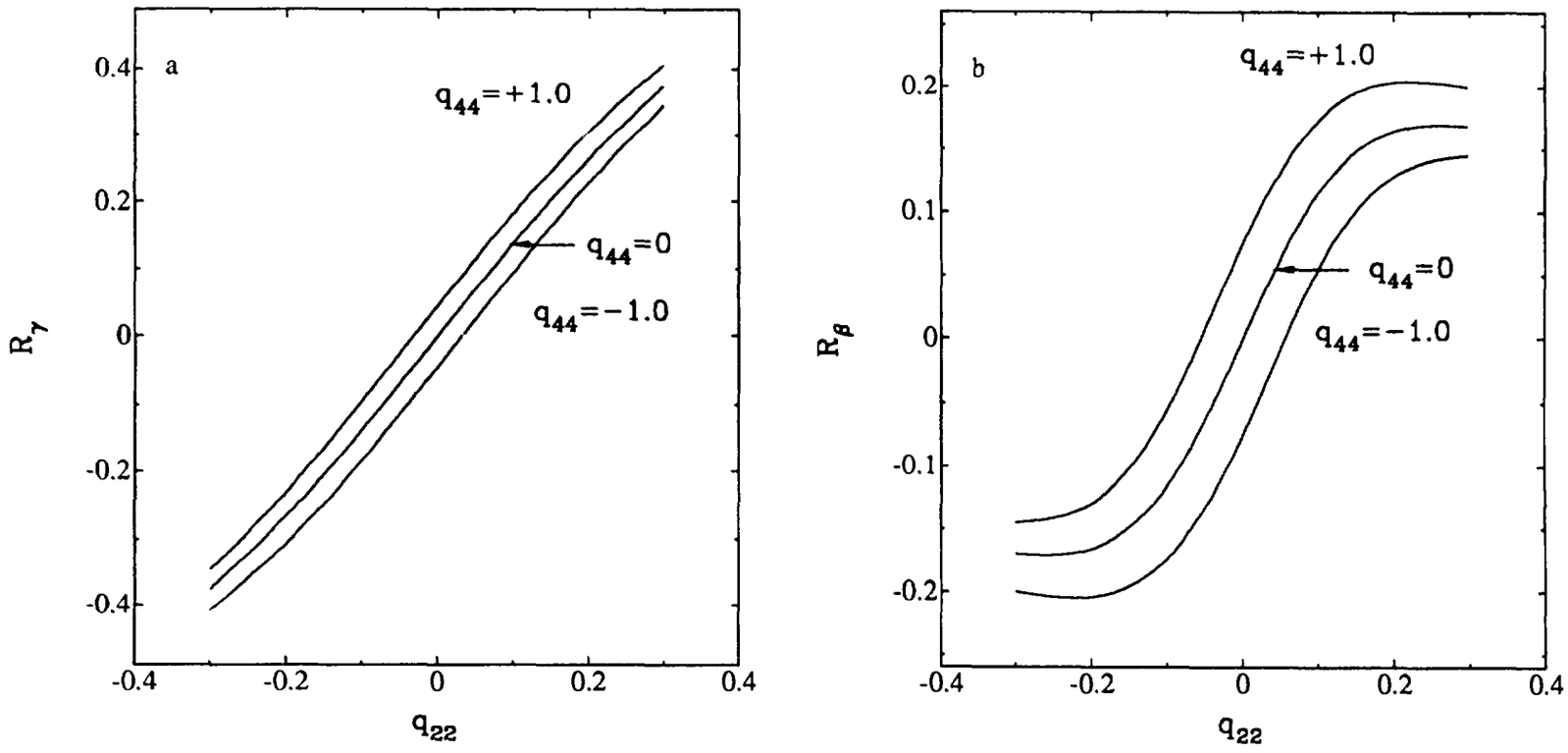
a
q_{44}=+1.0
q_{44}=0
q_{44}=−1.0
R_γ
q_{22}
0.4
0.2
0
-0.2
-0.4
b
q_{44}=+1.0
q_{44}=0
q_{44}=−1.0
R_β
q_{22}
0.2
0.1
0
-0.1
-0.2
-0.4
-0.2
0
0.2
0.4

Fig. 4

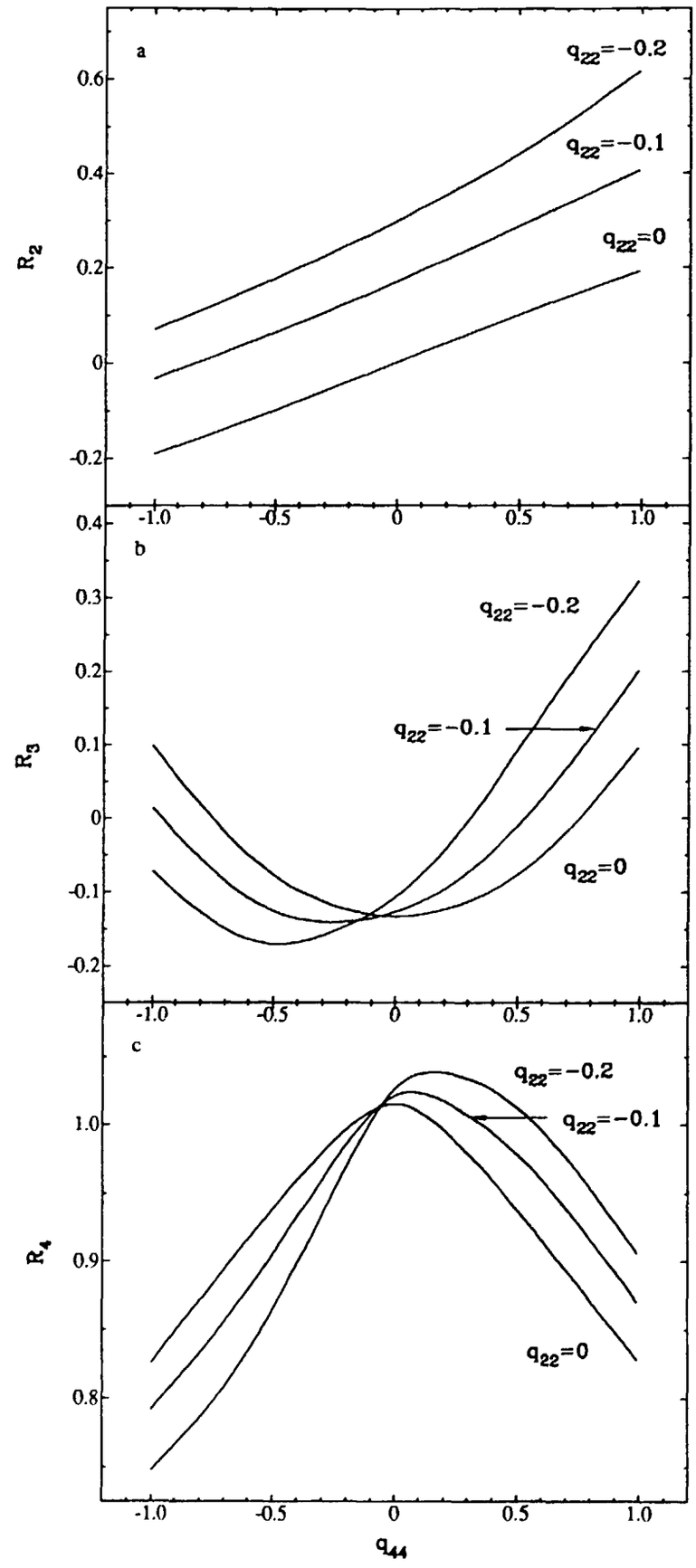
a
q_{22}=−0.2
q_{22}=−0.1
q_{22}=0
R_2
0.6
0.4
0.2
0
-0.2
-1.0
-0.5
0
0.5
1.0
b
q_{22}=−0.2
q_{22}=−0.1
q_{22}=0
R_3
0.3
0.2
0.1
0
-0.1
-0.2
c
q_{22}=−0.2
q_{22}=−0.1
q_{22}=0
R_4
1.0
0.9
0.8
q_{44}

Fig. 5

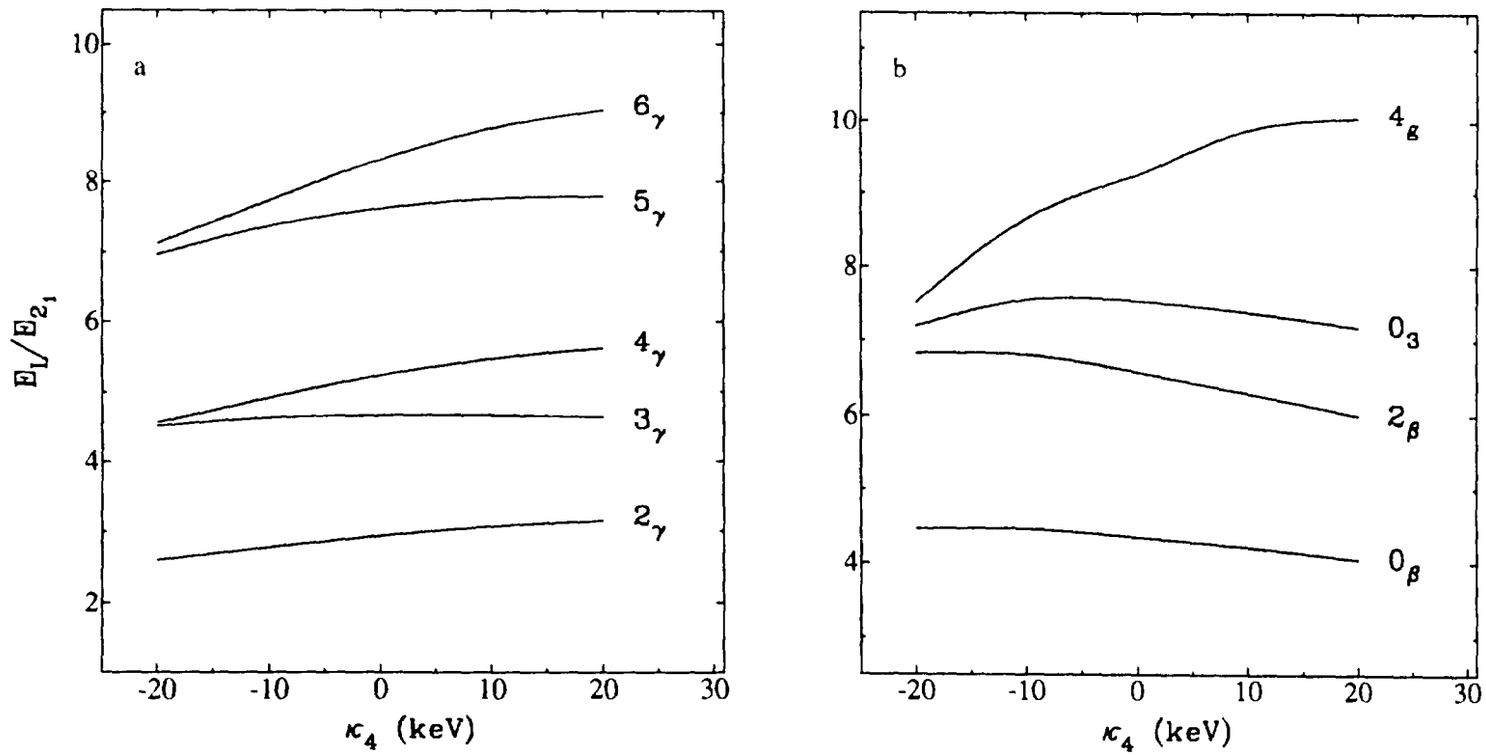
a
b
E_I/E_{2_1}
κ_4 (keV)
6_γ
5_γ
4_γ
3_γ
2_γ
4_g
0_3
2_β
0_β

Fig. 6

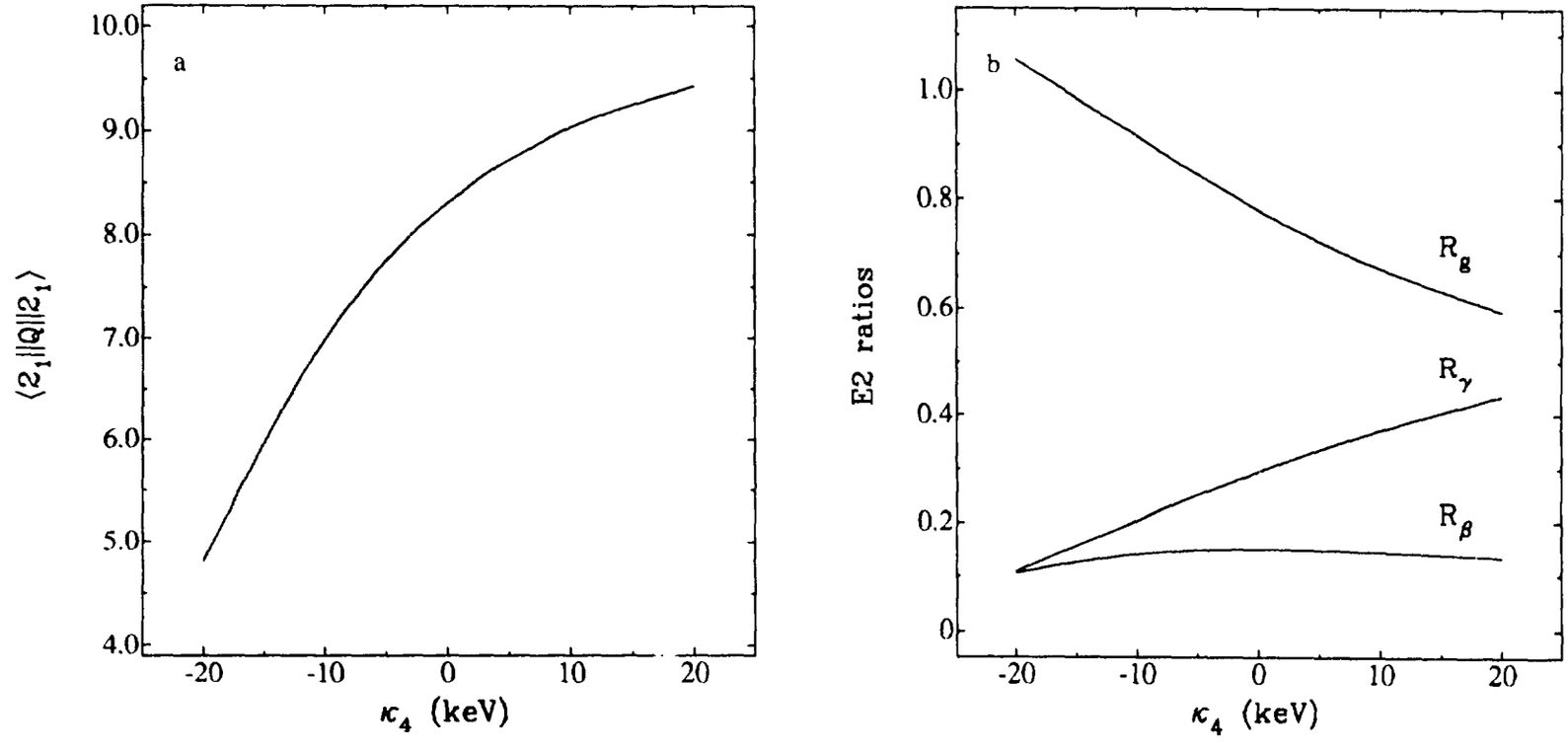
a
$\langle 2_1 \| Q \| 2_1 \rangle$
10.0
9.0
8.0
7.0
6.0
5.0
4.0
-20
-10
0
10
20
κ_4 (keV)
b
E2 ratios
1.0
0.8
0.6
0.4
0.2
0
R_g
R_γ
R_β
-20
-10
0
10
20
κ_4 (keV)

Fig. 7

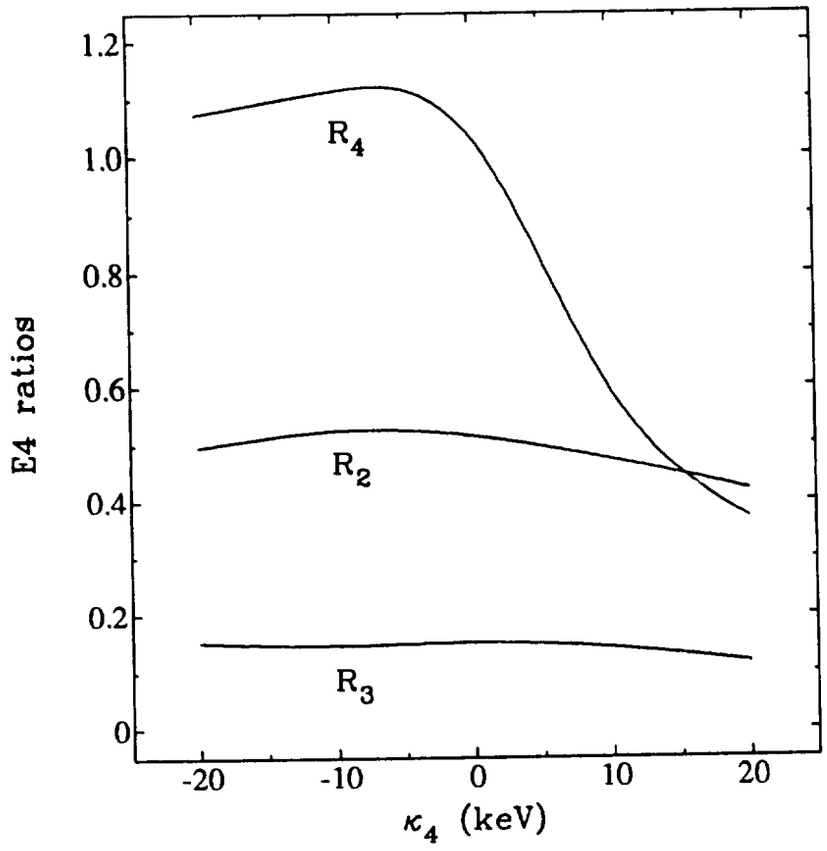

Fig. 8

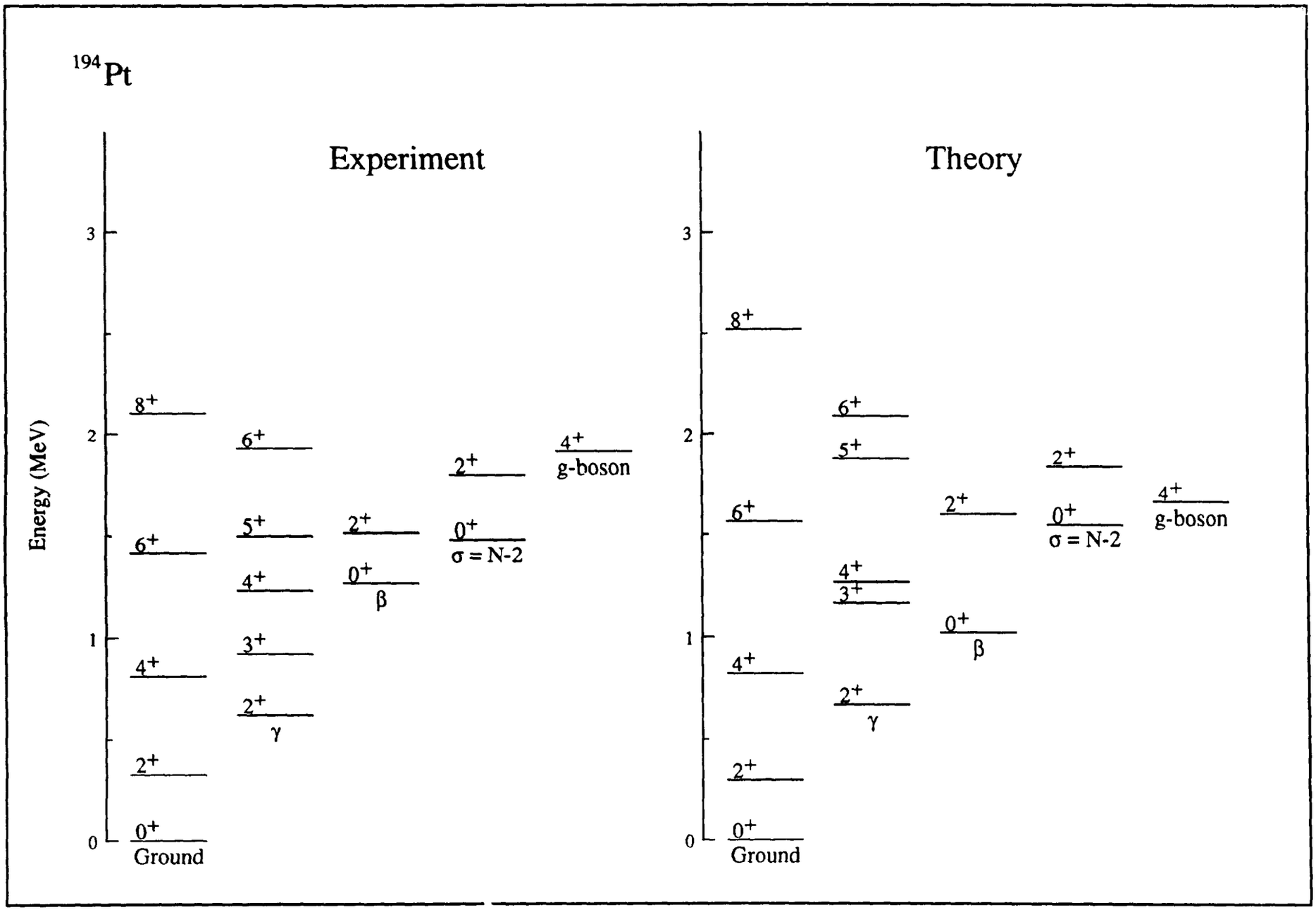
^{194}Pt
Experiment
Theory
Energy (MeV)
3
2
1
0
8^+
6^+
4^+
2^+
0^+
Ground
6^+
5^+
4^+
3^+
2^+
γ
2^+
0^+
β
2^+
0^+
σ = N-2
4^+
g-boson

Fig. 9

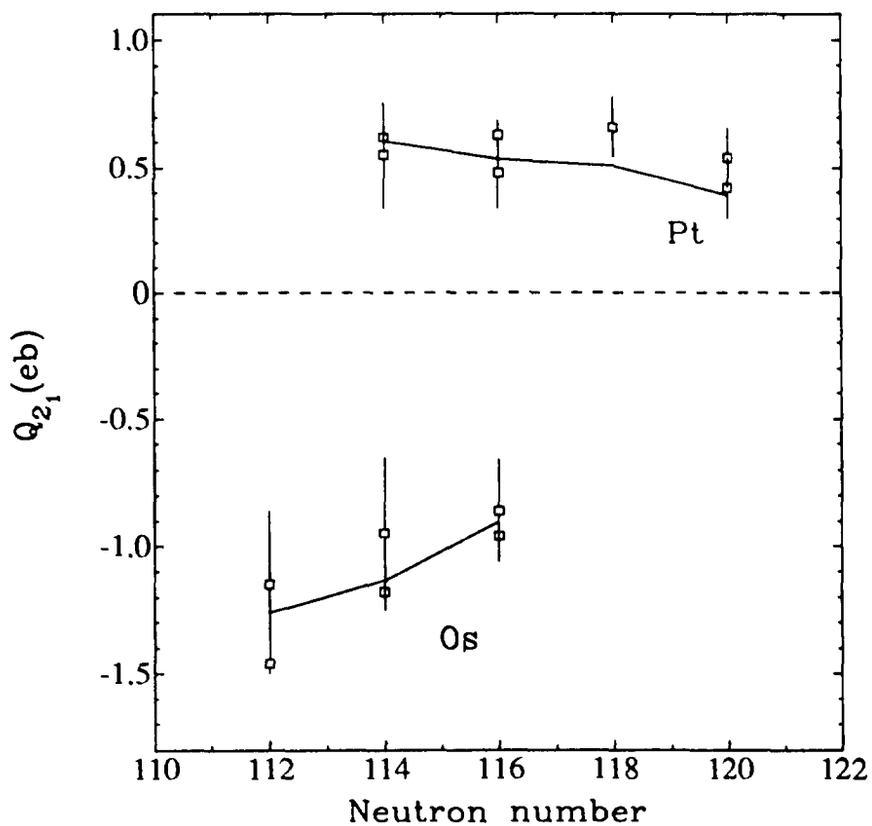
1.0
0.5
0
-0.5
-1.0
-1.5
Q_{2_1}(eb)
Pt
Os
110
112
114
116
118
120
122
Neutron number

Fig. 10

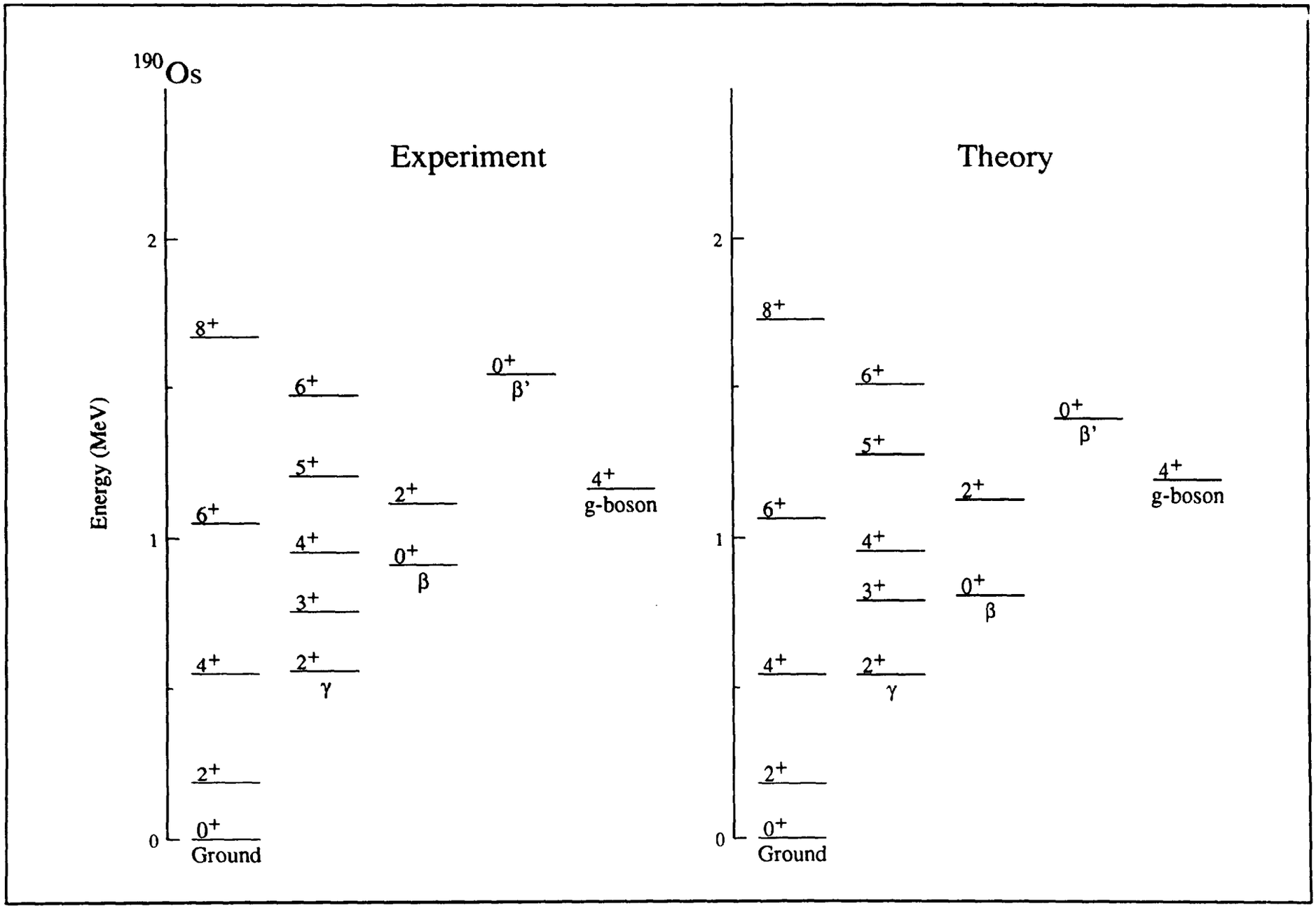
190Os
Experiment
Theory
Energy (MeV)
2
1
0
8+
6+
5+
4+
3+
2+
0+
Ground
γ
β
β'
g-boson

Fig. 11

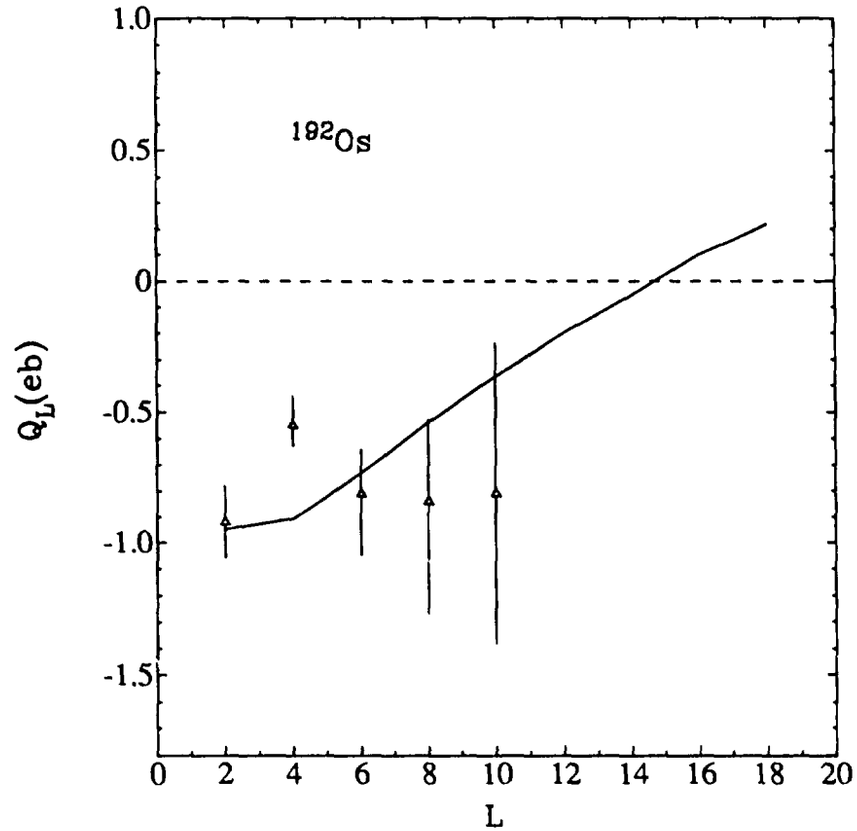

Fig. 12